

A VERY LARGE ARRAY RADIO-SURVEY OF EARLY-TYPE GALAXIES IN THE VIRGO CLUSTER

ALESSANDRO CAPETTI

INAF - Osservatorio Astronomico di Torino, Strada Osservatorio 20, I-10025 Pino Torinese, Italy

PREETI KHARB, DAVID J. AXON, DAVID MERRITT

Department of Physics, Rochester Institute of Technology, 85 Lomb Memorial Drive, Rochester, NY 14623, USA

AND

RANIERI D. BALDI

Università di Torino, via P. Giuria 1, 10125 Torino, Italy

Draft version November 8, 2018

ABSTRACT

We present the results of a 8.4 GHz Very Large Array radio survey of early-type galaxies extracted from the sample selected by Côté and collaborators for the Advanced Camera for Survey Virgo Cluster Survey. The aim of this survey is to investigate the origin of radio emission in early-type galaxies and its link with the host properties in an unexplored territory toward the lowest levels of both radio and optical luminosities. Radio images, available for all 63 galaxies with $B_T < 14.4$, show the presence of a compact radio source in 12 objects, with fluxes spanning from 0.13 to 2700 mJy. The remaining 51 galaxies, undetected at a flux limit of ~ 0.1 mJy, have radio luminosities $L \lesssim 4 \times 10^{18} \text{ WHz}^{-1}$. The fraction of radio-detected galaxies are a strong function of stellar mass, in agreement with previous results: none of the 30 galaxies with $M_* < 1.7 \times 10^{10} M_\odot$ is detected, while 8 of the 11 most massive galaxies have radio cores. There appears to be no simple relation between the presence of a stellar nucleus and radio emission. In fact, we find radio sources associated with two nucleated galaxies, but the majority of nucleated objects are not a radio emitter above our detection threshold.

A multiwavelength analysis of the active galactic nucleus (AGN) emission, combining radio and X-ray data, confirms the link between optical surface brightness profile and radio loudness in the sense that the bright core galaxies are associated with radio-loud AGNs, while non-core galaxies host radio-quiet AGNs. Not all radio-detected galaxies have a X-ray nuclear counter part (and vice-versa). A complete census of AGNs (and supermassive black holes, SMBHs) thus requires observations, at least, in both bands. Nonetheless, there are massive galaxies in the sample, expected to host a large SMBH ($M_{\text{BH}} \sim 10^8 M_\odot$), whose nuclear emission eludes detection despite their proximity and the depth and the spatial resolution of the available observations. Most likely this is due to an extremely low level of accretion onto the central SMBH.

Subject headings: galaxies: active, galaxies: clusters: individual: Virgo, galaxies: dwarf, galaxies: elliptical and lenticular, cD, radio continuum: galaxies

1. INTRODUCTION

Nuclear radio emission is almost invariably associated with the presence of an active galactic nucleus (AGN) and this is an indication that the process of accretion onto a supermassive black hole (SMBH) naturally produces a signature in the form of radiation in the radio domain. The separation between radio-loud (RL) and radio-quiet (RQ) AGNs is in fact only a measure of the relative flux in the radio band with respect to the optical or X-ray nucleus (Kellermann et al. 1994; Terashima & Wilson 2003); but also RQ AGNs, when studied at sufficient depth, usually show the presence at least of a nuclear radio component (e.g., Ulvestad & Wilson 1989; Nagar et al. 2005). For RL AGNs the radio core results from synchrotron emission produced by the unresolved base of their jets; for RQ AGNs the situation is more controversial and it has been recently proposed, besides the possibility of a jet origin, that their radio nuclei are the manifestation of the presence of a thermal outflow or of an active disk corona (Blundell & Kuncic 2007; Laor & Behar 2008)

When combined to the very limited effects that absorption has on radio waves, the study of radio emission provides, in principle, a very powerful tool to detect accretion onto SMBH and, consequently, to establish when a SMBH is present in

a given galaxy. However, to take full advantage of this approach, we must reach a much deeper understanding of what determines the radio luminosity of a given galaxy and how this is related to its level of accretion.

A large effort has been dedicated to explore the connection between the host properties (mostly from an optical point of view) and its radio emission. Already from the pioneering study by Auriemma et al. (1977) it was clear that more massive galaxies have on average a higher radio luminosity than smaller galaxies, while apparently there are no distinctions between clusters and non-clusters members (Ledlow & Owen 1996). The radio luminosity functions (RLFs) of galaxies of different optical magnitudes are similar but they differ strongly in their scaling. More recent studies confirm the early results, indicating that the normalization of the RLF scales with the host luminosity as $\sim L^{2.5}$ (e.g., Best et al. 2005; Mauch & Sadler 2007). However, galaxies of given optical magnitude show a very large range of radio power, more than 5 orders of magnitude, and the relation between the radio and optical luminosity can only be described in terms of a probability distribution.

These studies focused mostly on massive galaxies and had a relatively high threshold for the radio detection. The analysis

reaching the lowest level of luminosity (in both bands) were performed by Sadler et al. (1989) and Wrobel & Heeschen (1991), with limits at $L_r \sim 2.5 \times 10^{19} \text{ WHz}^{-1}$ and $M_r \sim -18.5$. Consequently, the information on the radio properties of galaxies of lower mass is sparse and incomplete. Similarly, there is still a dominant fraction of massive galaxies ($\sim 70\%$) undetected in radio surveys, for which only an upper limit to their radio luminosity can be derived.

Clearly, a survey reaching lower radio and optical luminosities can provide new insights on the origin and properties of the radio emission of early-type galaxies. The Virgo cluster represents a unique laboratory for such studies. In fact, it includes hundreds of early-type galaxies, spanning a wide range of stellar masses, for which a vast suite of data is available in the literature. In particular, the recent *Hubble Space Telescope* (*HST*) survey performed by Côté et al. (2004) provides us with a detailed analysis of their optical brightness profiles whose properties, including the presence of a stellar nucleus, can be included in the study of their radio emission. Given its proximity, its members can be observed at high spatial resolution ($1''$ at a distance of 17 Mpc corresponds to ~ 80 pc) and their nuclear emission can be studied down to extremely low luminosity level. For this reason we performed a radio survey of 63 early-type galaxies in Virgo with the Very Large Array (VLA). Since the aim of these observations is to explore their nuclear properties, the data were taken at high resolution (with the telescope in the A array configuration) and at relatively high frequency (8.4 GHz).

The paper is organized as follows. In Section 2 we describe the sample and the VLA observations; in Section 3 we discuss the link between the radio properties of the galaxies considered with their stellar mass, with their optical brightness profile and with the presence of a stellar nucleus; we then perform an analysis of the multiwavelength properties of their nuclear emission, taking advantage of X-ray data taken from the literature. Summary and conclusions are given in Section 4.

2. SAMPLE SELECTION AND VLA OBSERVATIONS

We considered initially the same sample selected by Côté et al. (2004) for their *HST* survey of early-type galaxies in the Virgo cluster. More specifically, they selected early-type galaxies from the VCC catalog (Binggeli et al. 1987) that consists of 2096 galaxies within this $\approx 140 \text{ deg}^2$ region. A total of 1277 VCC galaxies were considered by Binggeli et al. (1987) to be members of Virgo and for 403 cluster members radial velocities are available. A faint-end cutoff at $B_T < 16$ yields 352 galaxies, 163 of which are early-type galaxies according to the VCC morphological classifications of Binggeli et al. (1985). A subset of 100 early-type galaxies was then selected for observations with Advanced Camera for Survey (ACS) on *HST*, excluding objects with uncertain morphologies, lacking a clearly visible bulge component, with the presence of strong dust lanes, or signs of strong tidal interactions.

Of the 100 galaxies in the ACS Virgo cluster survey, high-quality radio data already exist for seven sources, all of them within the top third in terms of optical luminosity. We observed with the VLA additional 56 galaxies, in order of decreasing B_T band magnitude, for a total of 63 objects reaching $B_T = 14.4$.

2.1. VLA observations and data reduction

The galaxies were observed at 8.4 GHz with the VLA in the A-array configuration on 2006 April 17. The source scans, which were each ~ 30 minutes long, were interspersed with ~ 2 minutes scans of the nearby phase calibrator, 1239+075. 3C286 was used as the flux density calibrator for the experiment. The data were reduced using the standard calibration and reduction procedures in the Astronomical Image Processing System (AIPS). After the amplitude and phase calibration using the calibrators, the sources were split from the main data set and imaged using the task IMAGR. The detected radio sources were weak and were therefore not self-calibrated.

The resolution of the radio images is typically around $0''.3 \times 0''.2$, corresponding to a linear size of ~ 20 pc at the distance of Virgo. The typical resulting rms in the radio images is $30 \mu\text{Jy beam}^{-1}$. Five objects were detected with a peak to rms ratio larger than 5, and radio fluxes of these galaxies are reported in Table 1, together with the radio core measurements of the 7 radio galaxies found in the literature.

Radio images of these five sources are reproduced in Figure 1. The radio structures are typically unresolved and core-like; the exception is VCC1030, which appears elongated over $\sim 0''.2$ approximately along the direction of its large-scale dusty disk. The position of the radio source is always within less than $0''.8$ from the galaxy's center as measured in the *HST* images, and consistent with being coincident with it considering the uncertainties in the relative astrometry.

None of the observed galaxies is detected in the FIRST survey (with a limiting point source flux density of ~ 1 mJy) with the exceptions of VCC 1535, VCC 1154, VCC 1030, that are also seen in our images. For the undetected sources we provide the corresponding upper limits in Table 2.

3. RESULTS

3.1. Radio emission and host stellar mass

In Figure 2, left panel, we show the 3.6 cm radio luminosity of the VCC sources against their stellar masses, estimated using the recipe of Bell et al. (2007)

$$\log(M_*/L_{g_0}) = 0.698(g_0 - z_0) - 0.367$$

where g_0 and z_0 are the extinction corrected Sloan Digital Sky Survey (SDSS) total magnitudes. We adopted the distances estimated by Mei et al. (2007) from the analysis of the surface brightness fluctuations (see Table 1) and set the radio upper limits at 3 times the rms noise in the images. The typical radio flux limit of ~ 1 mJy corresponds to a radio luminosity of $L \sim 4 \times 10^{18} \text{ WHz}^{-1}$.

The radio detections are concentrated at the high end of the mass distribution, with no detections for the 30 galaxies with $M_* < 1.7 \times 10^{10} M_\odot$ (or $M_B > -18.6$). The fraction of detected galaxies increases with increasing stellar mass (Figure 2, right panel), reaching $\sim 70\%$. This is qualitative agreement with previous results on the bivariate radio-optical luminosity function of early-type galaxies that show that the fraction f of galaxies brighter than a given radio luminosity L is a strong function of the host mass, i.e. $f \propto M_*^{2.0-2.5}$ (e.g., Best et al. 2005; Mauch & Sadler 2007).

More quantitatively, we estimated the number of objects of our sample expected to be detected, assuming that the Best et al. (2005) probability law, derived from SDSS selected galaxies, can be extended to our regime of lower masses and radio-luminosities. We computed the probability of a radio detection for each source and derived the number of expected detections up to a given host mass. At the low

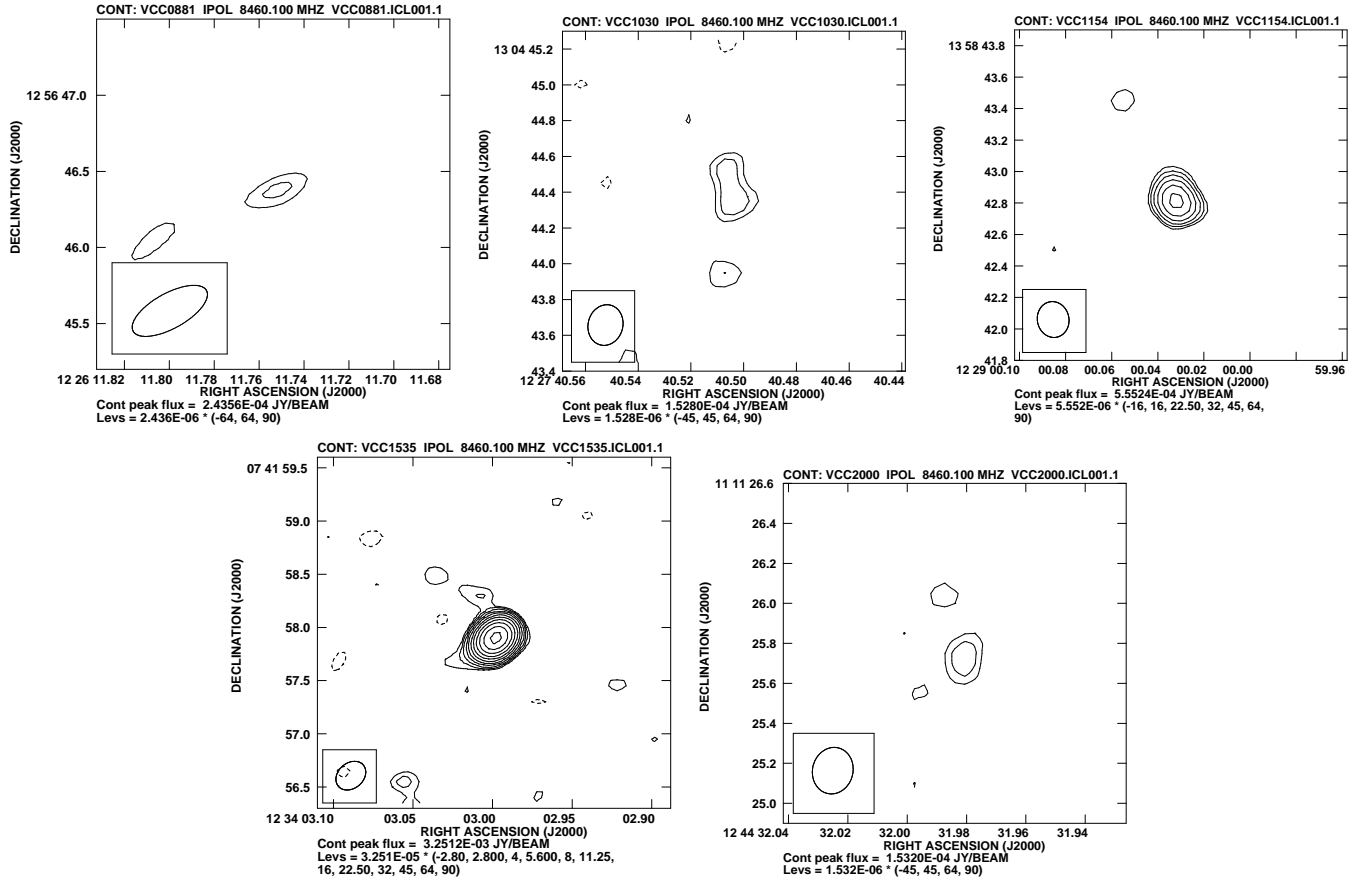


FIG. 1.— VLA 8.4 GHz radio maps of the five detected sources. The beam size is reported in the bottom left inset. All sources are consistent with being unresolved, with the exception of VCC1030, which appears elongated.

TABLE 1
PROPERTIES OF THE RADIO-DETECTED GALAXIES

Name	Alt. Name	B_T	D	$\log M_*$	F_{core}	$F_{1.4\text{GHz}}$	Prof.	Nuc.
VCC 1226	NGC 4472, M 49	9.31	17.14	12.0	3.7^b	256	cS	II
VCC 1316	NGC 4486, M 87	9.58	17.22	11.8	2726^b	226000	cS	0
VCC 1978	NGC 4649, M 60	9.81	17.30	11.7	18.4^c	29	cS	II
VCC 0881	NGC 4406, M 86	10.06	16.83	11.9	0.25^a	$< 1^d$	cS	II
VCC 0763	NGC 4374, M 84	10.26	18.45	11.7	180.7^b	6100	cS	II
VCC 1535	NGC 4526	10.61	16.52	11.0	3.27^a	12.00^d	cS ^e	0
VCC 1632	NGC 4552, M 89	10.78	15.85	11.3	58.1^b	100	cS	II
VCC 2095	NGC 4762	11.18	16.52	10.6	1.3^b	$< 1^d$	S	Ib
VCC 1154	NGC 4459	11.37	16.07	10.9	0.57^a	1.83^d	S	Id
VCC 1030	NGC 4435	11.84	16.75	10.6	0.14^a	2.16^d	S ^e	0
VCC 2000	NGC 4660	11.94	15.00	10.4	0.13^a	$< 1^d$	S	Id
VCC 1619	NGC 4550	12.50	15.49	10.2	0.7^b	$< 1^d$	S	Ia

Notes. Column description: (1) VCC name; (2) alternative optical identification; (3) B_T magnitude; (4) distance (Mpc); (5) total stellar mass in solar units; (6) 8.4 GHz radio-core flux (mJy) from (a) present work, and at 5 GHz from (b) Nagar et al. (2005), (c) Stanger & Warwick (1986); (7) total 1.4 GHz radio flux (mJy) from Condon et al. (1990, 2002), or ^d from the FIRST survey; (8) brightness profile classification: cS, core-Sérsic; S, Sérsic; ^e classification from our analysis of the *HST*/NICMOS images (see the Appendix); (9) nucleation classes: II, non-nucleated; 0, no classification possible; Ia and Ib: nucleated, Ic, and Id uncertain nuclei.

TABLE 2
THE RADIO UNDETECTED GALAXIES

Name	B_T	F_{core}^a	Name	B_T	F_{core}^a	Name	B_T	F_{core}^a	Name	B_T	F_{core}^a
VCC0798	10.09	0.11	VCC1938	12.11	0.10	VCC1146	12.93	0.08	VCC1871	13.86	0.09
VCC0731	10.51	0.10	VCC1279	12.15	0.15	VCC1025	13.06	0.09	VCC0009	13.93	0.08
VCC1903	10.76	0.10	VCC1720	12.29	0.11	VCC1303	13.10	0.09	VCC0575	14.14	0.08
VCC1231	11.10	0.13	VCC0355	12.41	0.10	VCC1913	13.22	0.09	VCC1910	14.17	0.12
VCC1062	11.40	0.08	VCC1883	12.57	0.10	VCC1327	13.26	0.17	VCC1049	14.20	0.17
VCC2092	11.51	0.08	VCC1242	12.60	0.09	VCC1125	13.30	0.10	VCC0856	14.25	0.10
VCC0369	11.80	0.08	VCC0784	12.67	0.08	VCC1475	13.36	0.26	VCC0140	14.30	0.08
VCC0759	11.80	0.07	VCC1537	12.70	0.08	VCC1178	13.37	0.14	VCC1355	14.31	0.08
VCC1692	11.82	0.07	VCC0778	12.72	0.08	VCC1283	13.45	0.13	VCC1087	14.31	0.08
VCC0685	11.99	0.09	VCC1321	12.84	0.08	VCC1261	13.56	0.12	VCC1297	14.33	0.15
VCC1664	12.02	0.09	VCC0828	12.84	0.08	VCC0698	13.60	0.11	VCC1861	14.37	0.10
VCC0654	12.03	0.11	VCC1250	12.91	0.08	VCC1422	13.64	0.10	VCC0543	14.39	0.10
VCC0944	12.08	0.10	VCC1630	12.91	0.08	VCC2048	13.81	0.09			

^a 3σ upper limits in mJy.

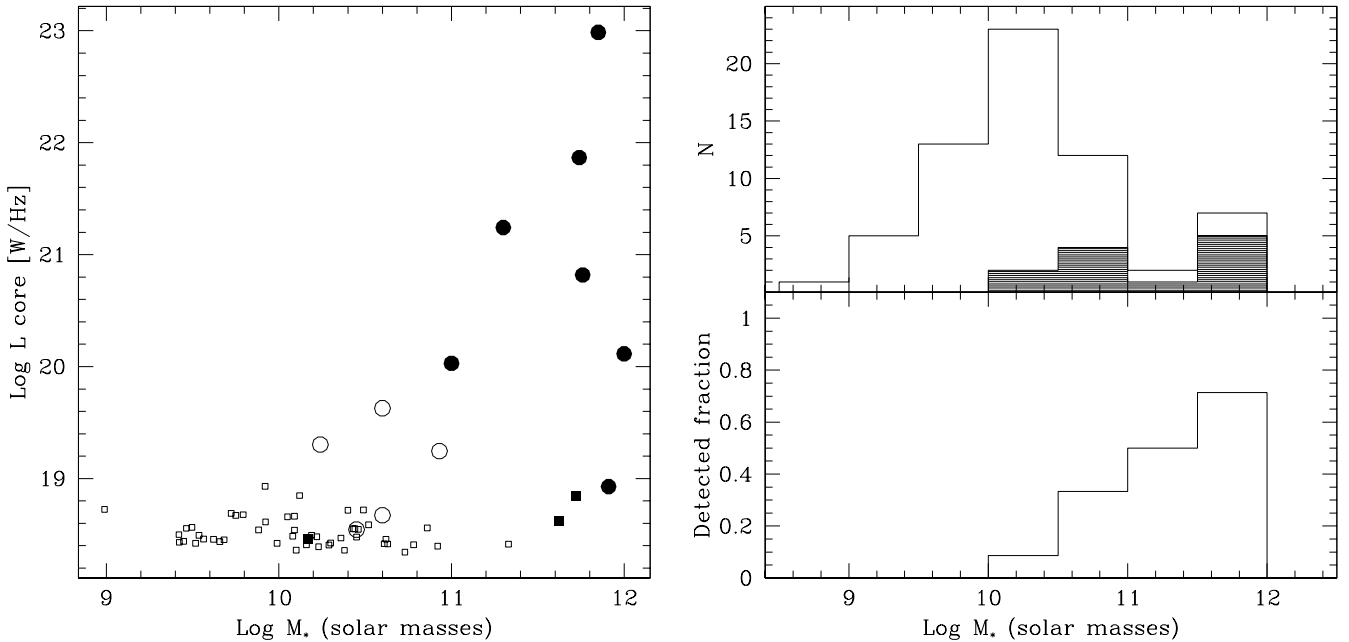


FIG. 2.— Left: radio core luminosity vs stellar masses. The radio detected galaxies are marked with large circles, separating them on the basis of the optical surface brightness profiles: filled circles are core galaxies, while empty circles are pure Sérsic galaxies. The undetected objects are marked with small squares (for clarity, we omit the downward pointing arrows), empty for Sérsic galaxies, filled for core galaxies. Right-top panel: distribution of stellar masses for the whole sample (empty histogram) and for the detected sources (filled histogram); bottom panel: fraction of detected sources vs. stellar mass in 0.5 dex bins.

mass end this predicts the detection of 0.06 sources up to $M_* < 1.7 \times 10^{10} M_\odot$, in agreement with the lack of radio detections in the 30 fainter galaxies of the sample. Considering now the high end mass, the probability law saturates to 100% at $M_* \sim 10^{11} M_\odot$, implying that all galaxies above this level are expected to be seen at the depth of our radio images. This is not the case since we have three radio undetected, optically bright, galaxies. Previous studies, characterized by far higher radio luminosity thresholds concur that a saturation of the detection rate at a $\sim 30\%$ level occurs at the high mass end (e.g., Mauch & Sadler 2007). Not surprisingly, expanding the radio luminosity coverage downward by 4 orders of magnitude we reach a higher detection rate, $\sim 70\%$. Nonetheless, we still have three bright galaxies without a radio source associated with them. These objects are $\gtrsim 30000$ times fainter than the radio core of M 87 (the brightest VCC galaxy) and at least $\gtrsim 200000$ times fainter in terms of total radio power, despite the similar stellar mass. This result emphasizes the probabilistic nature of the radio-optical bivariate law and that the optical luminosity of a given galaxy is not a good predictor of its level of radio emission.

3.2. Nucleation and radio emission

From the analysis of the data-set of *HST* images, Côté et al. (2006) found that a large fraction of VCC early-type galaxies is nucleated, with a frequency of 66% - 82%. Core galaxies do not follow this general rule, since they lack resolved stellar nuclei but, conversely, they often show unresolved optical nuclear sources (defined as nucleation class II). The origin of the nuclei in this class of galaxies, many of them associated with bright radio-sources, must be ascribed to the active nucleus and most likely they represent the synchrotron emission from the basis of their radio jets (Chiaberge et al. 1999; Balmaverde & Capetti 2006; Capetti et al. 2007).

We examine the possible presence of a link between nucleation and radio emission. Leaving aside the core galaxies, we are left with only five galaxies with a radio detection and a Sérsic profile. There are two clear nuclei (classes Ia and Ib), two uncertain nuclei (class Ic and Id), and a dusty galaxy (VCC1030) that cannot be classified from the point of view of nucleation (class 0). In the whole sample of 100 VCC the breakdown in terms of nucleation is 62:15:12:6 in the classes Ia-b:Ic-d:II:0 respectively¹.

The stronger connection between nucleation and radio properties is therefore the high incidence of radio nuclei in the core galaxies of the sample, lacking stellar nuclei. Leaving aside the core galaxies, the statistics is clearly very poor, but apparently there is no simple relation between nucleation and the detection of a radio source. In fact, we find radio sources associated with two certainly nucleated galaxies, but the majority of nucleated objects are not radio emitters above our detection threshold. Furthermore, the two nucleated galaxies for which we have a radio detection are among the brightest sources of our sample.

These results are consistent with the study by Seth et al. (2008) on the coincidence of nuclear star clusters and activity. They found that nucleated galaxies can host an AGN (thus a star cluster and an AGN are not mutually exclusive) and the fraction of nucleated active increases strongly with increasing galaxy mass. However, since this result applies also to the general population of galaxies, regardless of their nucleation,

¹ With an additional five sources of class Ie, reserved for compact sources offset from the galaxy center.

TABLE 3
COMPARISON OF X-RAY AND RADIO NUCLEAR LUMINOSITIES OF VCC GALAXIES WITH BOTH *Chandra* AND VLA OBSERVATIONS AVAILABLE.

Name	L_x (0.3 - 10 keV)	νL_ν	Profile
VCC 1226	<38.49	36.81	cS
VCC 1316	41.20	39.68	cS
VCC 1978	39.05	37.52	cS
VCC 763	39.73	38.57	cS
VCC 1632	39.58	37.94	cS
VCC 2095	38.71	36.33	S
VCC 0881	<38.64	35.85	cS
VCC 1535	<38.21	36.95	cS
VCC 1154	39.03	36.17	S
VCC 798	<38.43	<35.55	cS
VCC 731	39.00 ^a	<35.54	cS
VCC 1903	39.11	<35.34	S
VCC 1231	38.60	<35.48	S
VCC 2092	38.59	<35.32	S
VCC 1692	38.45	<35.34	S
VCC 685	39.14	<35.38	S
VCC 1664	39.95	<35.34	S
VCC 1720	<38.54	<35.48	S
VCC 1883	38.35	<35.47	S
VCC 1913	<38.46	<35.46	S
VCC 1178	38.67	<35.54	S
VCC 2048	<38.12	<35.38	S
VCC 9	<38.15	<35.38	S
VCC 1049	<38.08	<35.65	S
VCC 1297	38.42	<35.61	S

^a The identification of the brightest X-ray source with the AGN is uncertain (Sivakoff et al. 2003).

they concluded that the presence of a stellar nucleus is not linked to nuclear activity.

3.3. Host brightness profile and nuclear multiwavelength properties

The ACS/*HST* Virgo survey images were used by Ferrarese et al. (2006) to explore the properties of the surface brightness profiles (SBP) of the VCC galaxies. They found that, while the SBP are in general well described by a Sérsic (1968) model, in most of the brightest galaxies the inner profiles are lower than expected based on an extrapolation of the outer Sérsic law. These galaxies are better described by a core-Sérsic profile as defined by Trujillo et al. (2004)². Table 1 reports the complete list of optical classifications.³

Gallo et al. (2008) presented preliminary results of a program of *Chandra* observations of the VCC sample. They report the analysis of X-ray images for 32 objects, 25 in common with our sub-sample, and found X-ray nuclei in 16 galaxies, whose luminosities are given in Table 3. They conclude that these nuclear sources are most likely the manifestation of the presence of a low luminosity active nucleus. This opens the possibility of exploring the link between host brightness profile and AGNs multiwavelength properties.

² Also the low luminosity VCC 1250 is classified as a core-galaxy but this classification is considered as marginal and should be interpreted with caution since the galaxy morphology is severely affected by dust patches and a bright nuclear source.

³ In the Appendix we derive a classification of two galaxies of our sub-sample (VCC 1030 and VCC 1535) from new infrared *HST*. Their optical images are seriously contaminated by the presence of a large-scale dusty disk that prevent the study of the SBP.

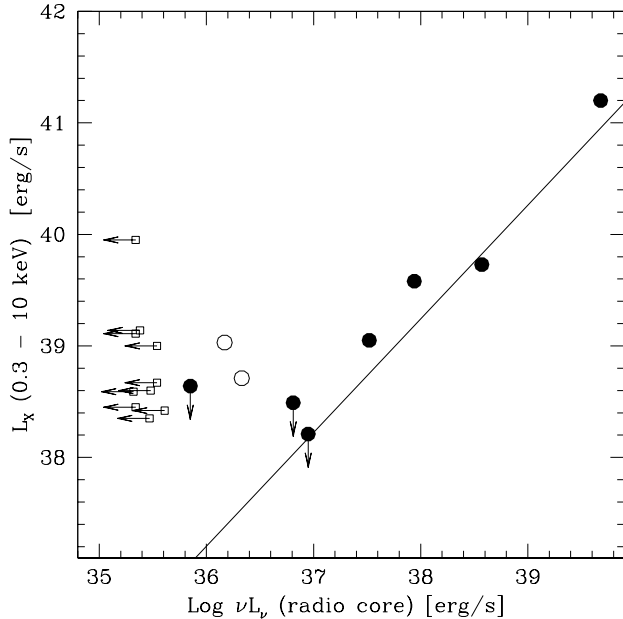


FIG. 3.— Comparison of radio and X-ray nuclear luminosities from Gallo et al. (2008). Filled circles are core galaxies and empty circles are Sérsic galaxies. The empty squares correspond to X-ray nuclei in galaxies not detected in our VLA survey. For clarity we do not show the objects that are upper limits both in radio and X-ray. The solid line represents the correlation of radio and X-ray luminosity for RL AGNs found by Balmaverde & Capetti (2006).

Chandra observations revealed an X-ray nucleus in five core galaxies, and all of them⁴ are consistent with the correlation linking radio and X-ray emission for RL AGNs derived by Balmaverde & Capetti (2006) (see Figure 3). Moving to the Sérsic galaxies, two have nuclei detected both in radio and X-ray, while 10 are only detected in the X-ray images. The location of these sources in the L_r versus L_X plane indicates that they are low luminosity RQ AGNs. These results confirm the relation between optical surface brightness profile and radio loudness (Capetti & Balmaverde 2006, 2007) in the sense that core galaxies are associated with RL AGNs, while non-core galaxies host RQ AGNs.

A consequence of these findings is that, not surprisingly, it is easier to detect the AGN emission in the radio band for a RL source and in the X-ray band for a RQ AGNs. This has an important consequence when we seek for a complete census of AGNs and consequently of SMBHs in a sample of galaxies, since only by combining radio and X-ray data it is possible to cover all AGNs manifestations. For example, the presence of an AGN in VCC 1226, the brightest cluster member, is not visible in X-ray images, while it is clearly shown by its radio images.

4. SUMMARY AND CONCLUSIONS

We presented the results of a radio survey of early-type galaxies in the Virgo cluster, extracted from the sample selected by Côté et al. (2004) for their ACS Virgo Cluster Survey. We observed 56 galaxies at 8.4 GHz with the VLA that, combined with data from the literature, provide radio images for all 63 galaxies brighter than $B_T = 14.4$. The aim of this survey is to investigate the origin of radio emission in early-type

⁴ With the only apparent exception of VCC 731. However, Sivakoff et al. (2003) stated that the identification of the brightest X-ray source with the AGN is uncertain.

galaxies and its link with the host properties in an unexplored territory toward the lowest levels of both radio and optical luminosities.

Compact radio sources are found in 12 objects, with fluxes from 0.13 to 2700 mJy. The remaining 51 galaxies are undetected at a flux limit of ~ 0.1 mJy, corresponding to radio luminosities $L \lesssim 4 \times 10^{18} \text{WHz}^{-1}$. The fraction of radio-detected galaxies is a strong function of stellar mass, in agreement with previous results on the bivariate radio/optical luminosity function of early-type galaxies: while none of the 30 galaxies with $M_* < 1.7 \times 10^{10} M_\odot$ is detected, 8 of the 11 most massive galaxies have radio cores. However, the galaxy mass is not a good predictor of its level of radio emission. This is clearly seen from a comparison of the radio properties of the brightest galaxies of the VCC. While they span only a factor of 10 in stellar mass, they cover a range of $\gtrsim 4.5$ orders of magnitude in radio-core power, and three of them are not detected in our radio images.

We note that VCC early-type galaxies with strong dust lanes or of signs of interactions were excluded by the original definition of the sample for the ACS Virgo cluster survey. Considering the links between mergers, dust content and nuclear activity suggested by previous studies of early-type galaxies (e.g., Tran et al. 2001; de Ruiter et al. 2002; Lauer et al. 2005) the sub-sample considered might be biased against active galaxies with respect to the overall population. This effect, however, does not affect the bright luminosity end, since the sample is complete down to $B_T = 12$.

We examined the possibility of a link between nucleation and radio emission. Core galaxies lack stellar nuclei and show a high incidence of radio nuclei. In the rest of the sample, only two nucleated galaxies show the presence of a radio source. Thus nuclear activity can coexist with a stellar nucleus, but the fraction of active galaxies is not related to nucleation.

We considered the properties of the surface brightness profiles, separating galaxies reproduced by a Sérsic law from those better described by a core-Sérsic profile. Furthermore, we relied on the results of X-ray *Chandra* observations by Gallo et al. (2008) to derive a multiwavelength view of the AGN emission. The reported link between optical surface brightness profile and radio loudness (Capetti & Balmaverde 2006) is found also in the VCC sample, since RL AGNs are associated with core galaxies, while non-core galaxies only host RQ AGNs.

Not all radio-detected galaxies have a X-ray nuclear counterpart, and vice-versa. Not surprisingly, it is easier to detect the AGN emission in the radio band for a RL source and in the X-ray band for a RQ AGNs. This has an important consequence when we seek for a complete census of AGNs and consequently of super-massive black holes for which a combination of (at least) radio and X-ray data is required.

Nonetheless, nuclear emission is not detected in a significant fraction of VCC galaxies in either observing band. Clearly, there is the possibility that the VCC sample crosses the minimum galaxy mass at which a SMBH is present (if such threshold indeed exists). However, there are no signs for the presence of an AGN in relatively massive VCC galaxies (e.g., VCC 798 and VCC 1720) despite the fact that they are expected to host a large SMBH ($M_{\text{BH}} \sim 10^8 M_\odot$), based on a typical ratio of 0.002 between SMBH and galaxy's mass (Marconi & Hunt 2003). This is particularly worrisome for a general use of AGNs as black-hole tracers, considering the proximity of the Virgo cluster, the depth and the spatial reso-

lution of the available observations.

In general, we cannot distinguish for the quiescent galaxies between a scenario 1) of a transition toward galaxies lacking a SMBH due to a low mass threshold, 2) the possibility that the SMBH has been ejected due to the recoil caused by the coalescence between two black holes following a galaxies merger (e.g., Campanelli et al. 2007), and 3) of extremely low accretion rate.

In fact, a crucial role in our ability to detect an active nucleus, and in setting its level of activity, is certainly played by the level of accretion onto the central SMBH. At least for low-power RL AGNs, it has shown that a suggestive linear correlation exists between the accretion rate of hot gas (estimated in a spherical approximation) and the jet power, over several orders of magnitude (Allen et al. 2006; Balmaverde et al. 2008). Therefore, to take full advantage of active nuclei as black hole tracers, it is necessary to combine a multiwavelength approach with estimates of the accretion rate. It is certainly of great interest to explore for example whether the

connection between the level of accretion and activity can be extended to the lowest level of radio emission seen in the RL VCC galaxies, and how this compares with similar estimates for RQ AGNs.

We thank the anonymous referee for his/her comments that help to improve the paper. The National Radio Astronomy Observatory is a facility of the National Science Foundation operated under cooperative agreement by Associated Universities, Inc. Based on observations obtained at the Space Telescope Science Institute, which is operated by the Association of Universities for Research in Astronomy, Incorporated, under NASA contract NAS 5-26555. This research has made use of the NASA/IPAC Infrared Science Archive, which is operated by the Jet Propulsion Laboratory, California Institute of Technology, under contract with the National Aeronautics and Space Administration.

REFERENCES

- Allen, S. W., Dunn, R. J. H., Fabian, A. C., Taylor, G. B., & Reynolds, C. S. 2006, *MNRAS*, 372, 21
- Auremma, C., Perola, G. C., Ekers, R. D., et al. 1977, *A&A*, 57, 41
- Balmaverde, B., Baldi, R. D., & Capetti, A. 2008, *A&A*, 486, 119
- Balmaverde, B. & Capetti, A. 2006, *A&A*, 447, 97
- Bell, E. F., Zheng, X. Z., Papovich, C., et al. 2007, *ApJ*, 663, 834
- Best, P. N., Kauffmann, G., Heckman, T. M., et al. 2005, *MNRAS*, 362, 25
- Binggeli, B., Sandage, A., & Tammann, G. A. 1985, *AJ*, 90, 1681
- Binggeli, B., Tammann, G. A., & Sandage, A. 1987, *AJ*, 94, 251
- Blundell, K. M. & Kuncic, Z. 2007, *ApJ*, 668, L103
- Campanelli, M., Lousto, C., Zlochower, Y., & Merritt, D. 2007, *ApJ*, 659, L5
- Capetti, A., Axon, D. J., Chiaberge, M., et al. 2007, *A&A*, 471, 137
- Capetti, A. & Balmaverde, B. 2006, *A&A*, 453, 27
- Capetti, A. & Balmaverde, B. 2007, *A&A*, 469, 75
- Chiaberge, M., Capetti, A., & Celotti, A. 1999, *A&A*, 349, 77
- Condon, J. J., Cotton, W. D., & Broderick, J. J. 2002, *AJ*, 124, 675
- Condon, J. J., Helou, G., Sanders, D. B., & Soifer, B. T. 1990, *ApJS*, 73, 359
- Côté, P., Blakeslee, J. P., Ferrarese, L., et al. 2004, *ApJS*, 153, 223
- Côté, P., Piatek, S., Ferrarese, L., et al. 2006, *ApJS*, 165, 57
- de Ruiter, H. R., Parma, P., Capetti, A., Fantì, R., & Morganti, R. 2002, *A&A*, 396, 857
- Ferrarese, L., Côté, P., Jordán, A., et al. 2006, *ApJS*, 164, 334
- Gallo, E., Treu, T., Jacob, J., et al. 2008, *ApJ*, 680, 154
- Jedrzejewski, R. I. 1987, *MNRAS*, 226, 747
- Kellermann, K. I., Sramek, R. A., Schmidt, M., Green, R. F., & Shaffer, D. B. 1994, *AJ*, 108, 1163
- Laor, A. & Behar, E. 2008, *MNRAS*, 390, 847
- Lauer, T. R., Faber, S. M., Gebhardt, K., et al. 2005, *AJ*, 129, 2138
- Ledlow, M. J. & Owen, F. N. 1996, *AJ*, 112, 9
- Marconi, A. & Hunt, L. K. 2003, *ApJ*, 589, L21
- Mauch, T. & Sadler, E. M. 2007, *MNRAS*, 375, 931
- Mei, S., Blakeslee, J. P., Côté, P., et al. 2007, *ApJ*, 655, 144
- Nagar, N. M., Falcke, H., & Wilson, A. S. 2005, *A&A*, 435, 521
- Sadler, E. M., Jenkins, C. R., & Kotanyi, C. G. 1989, *MNRAS*, 240, 591
- Sérsic, J.-L. 1968, *Atlas de Galaxias Australes* (Córdoba: Obs. Astron.)
- Seth, A., Agüeros, M., Lee, D., & Basu-Zych, A. 2008, *ApJ*, 678, 116
- Sivakoff, G. R., Sarazin, C. L., & Irwin, J. A. 2003, *ApJ*, 599, 218
- Stanger, V. J. & Warwick, R. S. 1986, *MNRAS*, 220, 363
- Terashima, Y. & Wilson, A. S. 2003, *ApJ*, 583, 145
- Tran, H. D., Tsvetanov, Z., Ford, H. C., et al. 2001, *AJ*, 121, 2928
- Trujillo, I., Erwin, P., Asensio Ramos, A., & Graham, A. W. 2004, *AJ*, 127, 1917
- Ulvestad, J. S. & Wilson, A. S. 1989, *ApJ*, 343, 659
- Wrobel, J. M. & Heeschen, D. S. 1991, *AJ*, 101, 148

APPENDIX

The optical images of two galaxies of the sample (namely VCC 1030 and VCC 1535) both detected in the VLA images, show the presence of large-scale dusty disks (Côté et al. 2004) that prevent the study and classification of their surface brightness profiles. We then retrieved from the *HST* archive their infrared images where the impact of dust absorption is less severe. The images were taken with NICMOS/*HST* through the filter F160W (*H* band) and were processed by the standard *HST* pipeline. The camera NIC1 was used, with a pixel size of $0''.043$, for a field of view of $\sim 11'' \times 11''$.

Elliptical isophotes were fit to both images using the IRAF task ‘ellipse’ (Jedrzejewski 1987). Although these images are still affected by dust absorption (see Figure 4 and 5), there are sufficient dust free regions to derive the SBP after proper masking. Since the image of VCC 1535 fills completely the field of view, we extended the radial coverage of the SBP using the *H* band image from the Two Micron All Sky Survey (2MASS).

The SBP were fit using a Sérsic law (Sérsic 1968) convolved with the appropriate point-spread function before comparison with the data. The SBP of VCC 1030 is reproduced very closely by a Sérsic model with an effective radius of $r_e = 3''.9$ and a Sérsic index $n = 1.7$. This is not the case of VCC 1535 that shows a strong light deficit in the innermost regions with respect to the Sérsic that describes the external regions and requires the presence of a flat central core. We therefore fit its SBP with a core-Sérsic model (Trujillo et al. 2004); the parameters of the best fit are an effective radius $r_e = 106''$, an index $n = 5.2$, a core radius $r_c = 0''.15$, and an inner slope $\gamma = 0.06$. This analysis leads to a classification based on the SBP properties of VCC 1030 as a Sérsic galaxy and of VCC 1535 as a core-Sérsic galaxy.

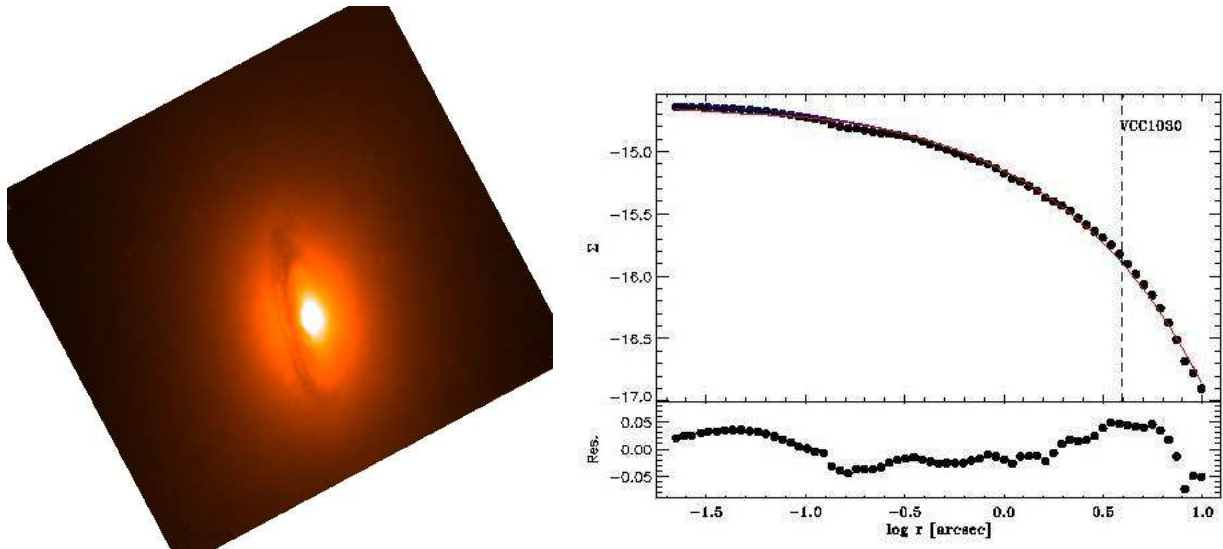


FIG. 4.— *HST*/NICMOS image of VCC 1030 and (on the right panel) the derived surface brightness profile. The solid line reproduces the best fit Sérsic law. The vertical dashed line marks the value of the effective radius, $r_e = 3.9''$. The vertical axis gives the logarithm of the surface brightness in unit of $[\text{erg s}^{-1} \text{cm}^{-2} \text{Å}^{-1} \text{arcsec}^{-2}]$. In the bottom inset we show the residuals of the fit.

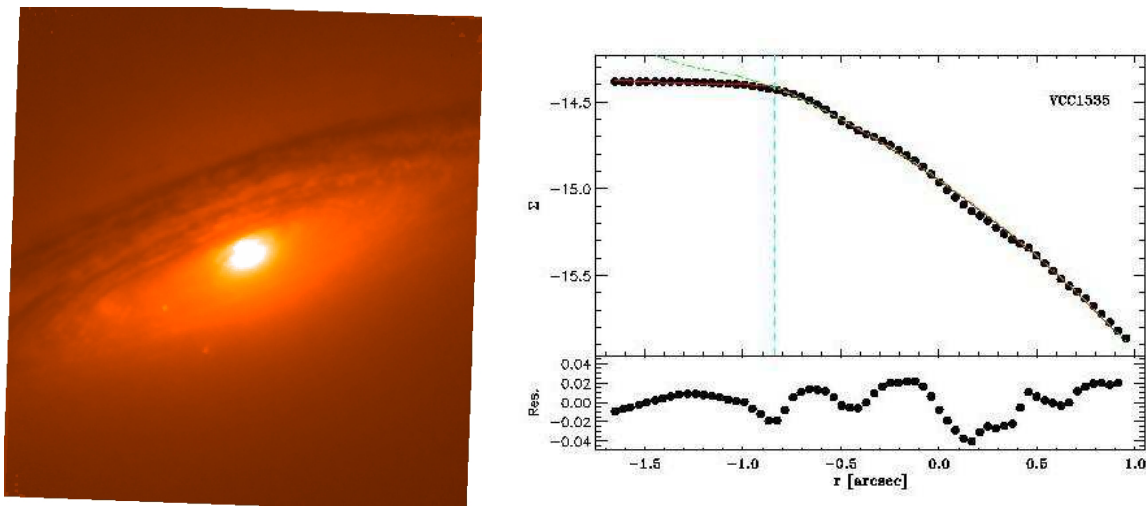


FIG. 5.— Same as Figure 4 for VCC 1535. The vertical dashed line marks the value of the core radius, $r_c = 0.''15$. The dot-dashed line is the best-fit Sérsic law to the external regions ($r > 1''$) of the galaxy, that overpredicts the central surface brightness.